On the Formation of Trapped Electron Radiation Belts at Ganymede

Lucas Liuzzo[1], Quentin Nénon[2], Andrew R. Poppe[1], Aaron Stahl[3,4], Sven Simon[3,4], and Shahab Fatemi[5]

[1]Space Sciences Laboratory, University of California, Berkeley, CA, USA
[2]Institut de Recherche en Astrophysique et Planétéologie, CNRS-Université Toulouse III-CNES, Toulouse, France
[3]School of Earth and Atmospheric Sciences, Georgia Institute of Technology, Atlanta, GA, USA
[4]School of Physics, Georgia Institute of Technology, Atlanta, GA, USA
[5]Department of Physics, Umeå University, Umeå, Sweden

Key Points:

- We compare Galileo G28 energetic electron data with test particle tracing to identify a population of trapped electrons at Ganymede
- We achieve a robust match between the energetic electron pitch angle distributions from our model compared to those observed by Galileo
- Electrons follow stable orbits that can encircle the moon multiple times before being lost to the surface or to Jupiter's magnetosphere

Corresponding author: Lucas Liuzzo, `liuzzo@berkeley.edu`

Abstract

This study presents evidence of stably trapped electrons at Jupiter's moon Ganymede. We model energetic electron pitch angle distributions and compare them to observations from the Galileo Energetic Particle Detector to identify signatures of trapped particles during the G28 encounter. We trace electron trajectories to show that they enter Ganymede's mini-magnetospheric environment, become trapped, and drift around the moon for up to 30 minutes, in some cases stably orbiting the moon multiple times. Conservation of the first adiabatic invariant partially contributes to energy changes throughout the electrons' orbits, with additional acceleration driven by local electric fields, before they return to Jupiter's magnetosphere or impact the surface. These trapped particles manifest as an electron population with an enhanced flux compared to elsewhere within the mini-magnetosphere that are detectable by future spacecraft.

Plain Language Summary

The magnetized planets of the solar system are known to possess a population of high-energy, orbiting electrons that are sustained for extended timescales. By comparison, Ganymede, the only moon in the solar system confirmed to have its own permanent magnetic field, should also retain a similar population of trapped particles. Observations from the Galileo mission hint at the existence of electrons that may be locally trapped at the moon, but information regarding their origin and the mechanism behind trapping these electrons is unknown. Furthermore, there are no constraints on the processes that help sustain such a trapped population, and the timescales over which they are maintained at Ganymede remain unknown. In this study, we provide evidence that trapped electrons exist at Ganymede, identify the mechanisms driving their dynamics, and answer open questions about the moon's local energetic particle environment.

1 Introduction

Ganymede, with a radius of $R_G = 2{,}634.1$ km, is the largest of Jupiter's moons and is the only moon in the solar system known to possess its own permanent magnetic field (e.g., Jia & Kivelson, 2021; Kivelson et al., 2002). The mini-magnetosphere formed by Ganymede's interaction with the ambient plasma largely prevents Jovian ions and electrons from reaching the moon's equatorial surface (e.g,. Allioux et al., 2013; Fatemi et al., 2016; Liuzzo et al., 2020; Plainaki et al., 2020), while allowing these particles ac-

cess to the polar hemispheres (e.g., Cooper et al., 2001; Paranicas et al., 2022; Poppe et al., 2018; Smith et al., 1979; Vorburger et al., 2022).

While sustained electron radiation belts have been observed at the magnetized outer planets (e.g., Mauk & Fox, 2010), and predicted at Mercury (Kollmann et al., 2022; Oran et al., 2022; Schriver et al., 2011), the role that Ganymede's permanent magnetic field has in accelerating, trapping, and maintaining an electron population with stable orbits is not well understood. Using data from the Galileo spacecraft's Energetic Particle Detector (EPD), Williams et al. (1997) found hints of energetic electrons that were quasi-trapped around Ganymede during the G8 encounter as Galileo passed through the moon's equatorial closed field line region. The distributions of these particles were characterized by decreases in counts at field-aligned and anti-field-aligned pitch angles (where electrons were within Ganymede's loss cone) and additional decreases near perpendicular pitch angles ($\alpha \approx 90°$) associated with magnetopause shadowing and drift shell splitting (where electrons were lost to the Jovian magnetosphere as they drifted around Ganymede; e.g., Roederer, 1967). The intensities at all other pitch angles were enhanced, resulting in the characteristic "butterfly" distribution of a quasi-trapped population comprised of particles in (partial) orbit around Ganymede during G8.

For the G28 encounter on 20 May 2000, Galileo also passed upstream of the moon and crossed into the closed field line region. Williams (2001) found that there were no losses for $\alpha \approx 90°$ pitch angle electrons as there were during G8. Instead, they displayed clear losses at field aligned and anti-aligned pitch angles during G28, indicating electrons may have possessed stably trapped orbits around Ganymede forming sustained radiation belts. Similar "pancake" distributions were observed during the G29 encounter as well (Williams, 2004). Despite these observations, the stability of, and the mechanisms for trapping this electron population remain unknown. Using data from Galileo as well as Juno, Kollmann et al. (2022) have recently confirmed that a radiation cavity exists within Ganymede's mini-magnetosphere (even though Juno did not cross into the closed field line region) and, using EPD data, have identified a region of enhanced electron phase space density (PSD) compared to this cavity, when traveling closer to the moon's surface at low Ganymede L-shells. These authors suggest that the enhanced fluxes may be indicative of an electron radiation belt surrounding the moon at low altitudes and provide first estimates regarding the stability of such a population. However, they did not consider the role that the moon's local environment has on the dynamics of these par-

ticles, and the mechanisms responsible for trapping and accelerating these electrons at Ganymede remains poorly constrained.

To investigate the role that these effects play at Ganymede, and to address the likelihood that electron radiation belts remain stably trapped at the moon along with their associated timescales, we compare energetic electron observations from EPD obtained during the Galileo spacecraft's G28 flyby to a particle tracing model. We focus on this flyby since, compared to the other Ganymede encounters, Galileo crossed the deepest into the closed field line region which shields Jovian magnetospheric particles from accessing the moon's local environment (e.g., Liuzzo et al., 2020; Plainaki et al., 2022), thereby providing the highest likelihood to detect electrons that may be trapped around Ganymede. We apply results from two independent models of Ganymede's electromagnetic environment to provide robust evidence for Galileo's detection of a trapped electron population that formed radiation belts at Ganymede during G28.

2 Modeling Ganymede's Magnetospheric Environment

To describe the three-dimensional structure of the electromagnetic environment near Ganymede, we apply the results for the G28 encounter from two different models, Fatemi et al. (2016) and Stahl et al. (2023b). These studies utilized separate hybrid simulation frameworks to model Ganymede's environment, in which low-energy ions are treated as individual particles but the low-energy electrons are represented as a massless, charge-neutralizing fluid within the models. While the initial conditions differ between these models (e.g., the Jovian magnetospheric field vector, ambient plasma number density, and Ganymede's magnetic moment; cf. Fatemi et al., 2016; Stahl et al., 2023b), each has been validated against data from multiple Galileo encounters and the magnetic field output from the simulations quantitatively match key features of the time series observed during G28. While slight differences between the modeled results exist (e.g., timing of Galileo's magnetopause exit or the fine-scale structure of the magnetic field components), applying results from two independent hybrid models allows us to investigate the robustness of our results when comparing to energetic electron data from Galileo EPD.

We apply the Galilean Energetics Tracing Model (GENTOo; see Liuzzo et al., 2019a, 2019b, 2022) to trace energetic electrons through Ganymede's perturbed electromagnetic environment as modeled by the hybrid simulations. The hybrid model outputs represent

a snapshot at a given point in time after they reach a quasi-steady state; thus, the GENTOo results do not take into account, e.g., scattering of electrons by Kelvin Helmholtz waves that travel along Ganymede's magnetopause (e.g., Stahl et al., 2023b). Since GENTOo has been described in detail by Liuzzo et al. (2020, 2024) for studying electrons at Ganymede and for comparing results to Galileo EPD data, only a brief description will be provided here. GENTOo traces particles backward in time (i.e., with a time step $\mathrm{d}t < 0$) using a relativistic solver for their equation of motion. Compared to other energetic particle tracing models that have been applied to Ganymede, GENTOo is the only framework that captures the electrons' bounce motion through the Jovian magnetosphere and their return to Ganymede's vicinity (potentially) multiple times, by using an analytical approach (Roederer, 1967). Energetic electrons can leave the local environment, travel to high Jovian magnetic latitudes, mirror, and return on timescales of seconds (Liuzzo et al., 2020), so such an approach is important to accurately model their access to Ganymede. One of two outcomes can occur for each electron back-traced with GENTOo, resulting in either an "allowed" or "forbidden" trajectory. A forbidden trajectory occurs whenever the electron's position r intersects Ganymede's surface; in a forward-tracing approach, such a particle would be required to travel through the moon to reach the point at which the (back-traced) particle was initialized in GENTOo. These particles are nonphysical and are removed from the simulation. Alternatively, particles with allowed trajectories never encounter Ganymede when integrating backward in time, even after multiple bounces through the Jovian magnetosphere. Electrons are allowed when they travel beyond the upstream or downstream face of the hybrid simulation domain where the electromagnetic fields have returned to their background values (see Fatemi et al., 2016; Stahl et al., 2023b). For these electrons, GENTOo applies Liouville's theorem to convert the flux observed at their energy in the ambient magnetospheric plasma to the flux they carry at a given location in the interaction region (in this case, Galileo and the EPD).

To compare to the EPD electron observations, we proceed analogous to Liuzzo et al. (2024) and average the observed electron pitch angle distributions (PADs) over a full sweep of the EPD stepper motor, an approximately two-minute period during which the instrument sampled a full 4π sr field of view. We exclude all times when the EPD motor was at position 0, since those counts are reduced by the instrument background shield (see Kollmann et al., 2022), but we keep fluxes from motor position 7 for this study. Data from EPD's Low Energy Magnetospheric Measurements System are not affected by anoma-

lous drops in energetic particle counts associated with this motor position (see also Nénon, 2022). This averaging results in a discretization of the G28 flyby trajectory into 31 positions (each corresponding to Galileo's location at the center of each averaging window), from which we initialize electrons at an energy of $E = 21$ keV, corresponding to the center energy of the E0 channel (sensitive to electrons from $15 \leq E \leq 29$ keV). At each point, electrons are launched isotropically with a resolution of 1° in pitch angle and 2° in gyrophase.

3 Results

Figure 1 displays the G28 trajectory along with the electron PAD measured in the EPD E0 channel (see also, e.g., Kollmann et al., 2022; Nénon et al., 2022; Williams, 2001). The apparent dropouts in the data for which there are no measured fluxes (white spaces in panel 1c) correspond to pitch angles that were not sampled by EPD at that time. For the ~ 40 minutes prior to closest approach of Ganymede, the electrons displayed characteristics of a "scattered-beam" distribution, where fluxes near aligned and anti-aligned pitch angles were enhanced, but with a distribution that still included non-zero fluxes at more perpendicular pitch angles. Mauk and Saur (2007) suggested that, because these scattered beams were observed far outside of Ganymede's mini-magnetosphere (at distances of up to $5R_G$ where the moon's influence on energetic electrons should be minimal), they were likely not associated with Ganymede. Instead, they state that the beams may have been driven by processes in the Jovian magnetosphere (see also Nénon et al., 2022).

Within $\sim$ 3 minutes of closest approach (C/A), Galileo detected a clear feature related to Ganymede's interaction in EPD data. Near 10:06 UTC, after Galileo entered Ganymede's closed field line region, where the differential electron energy flux was $\sim 80\%$ lower than the value outside of Ganymede's mini-magnetosphere and focused near pitch angles of $\alpha \approx 90°$. The flux away from 90° was decreased by nearly two orders of magnitude compared to the ambient Jovian magnetosphere. This pancake PAD suggests trapped particles: electrons near $\alpha = 0°$ and $\alpha = 180°$ are within the loss cone and impact Ganymede's surface, whereas particles with more perpendicular pitch angles mirror in the enhanced field (see also Williams, 2001). Figure 1d displays the same electron PAD, but with the fluxes in each time segment (i.e., the full pitch angle range over each sweep of the EPD stepper motor) normalized to the maximum flux measured at that time. Here, the beamed

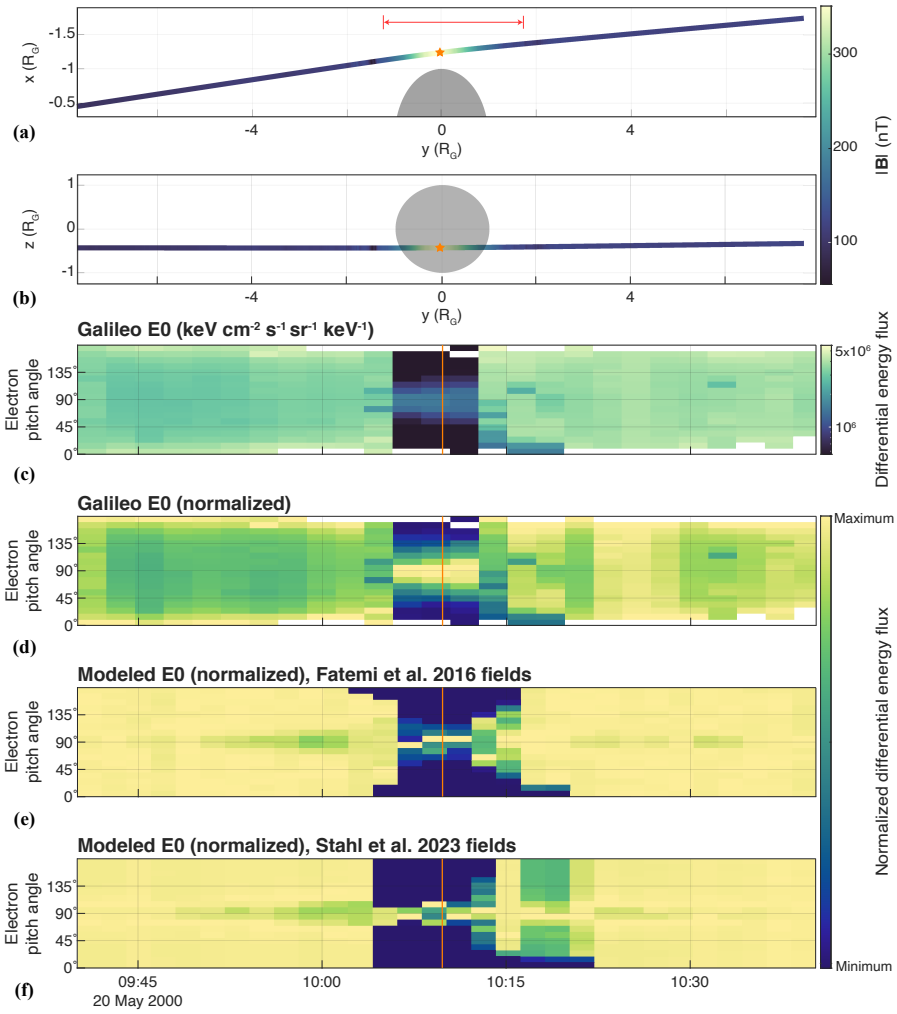

Figure 1. Galileo measurements during G28 and associated model results. Panels (a) and (b) display the trajectory in the $z = 0$ and $x = 0$ planes of the GphiO coordinate system (x along corotation, z northward), respectively, colored corresponding to the magnitude of the observed magnetic field. Ganymede is represented in gray. Panels (c–d) display the electron PAD from the EPD E0 channel, (c) in units of differential energy flux or (d) normalized to the maximum value of each time bin. Panels (e–f) show results from GENTOo, using fields from Fatemi et al. (2016) or Stahl et al. (2023b), respectively. The temporal position of each bin in panels (c–f) corresponds to the spatial position of Galileo in panels (a) and (b). Orange stars and vertical lines denote C/A, while the red horizontal line in panel (a) indicates the closed magnetic field line region (Kivelson et al., 2002; Williams, 2001).

distribution before closest approach and the relative enhancement in flux near $\alpha \approx 90°$ within Ganymede's magnetosphere are even more apparent than in panel 1c. Although Figures 1c–d only include data from the EPD E0 channel, similar signatures within the closed field line region were detected at nearly all EPD energies, extending beyond $E >$ 1 MeV during G28 (see Kollmann et al., 2022; Nénon et al., 2022; Williams, 2001).

Figures 1e–f show the results from GENTOo for electrons at energies $E = 21$ keV initialized and traced backward in time from the G28 trajectory using the two different hybrid model results (Fatemi et al., 2016; Stahl et al., 2023b). For both sets of electromagnetic field conditions, the model predicts a pancake electron PAD that agrees well with the observations: clear bite-outs at field-aligned and anti-field-aligned pitch angles are formed before and after C/A, while a population of electrons with pitch angles $60° \lesssim \alpha \lesssim 120°$ persists. Although we focus only on the EPD E0 channel, our modeling indicates similar electron distributions for all energies detectable by EPD (beyond 1 MeV). The observed PAD within this region is smoother than the model output, which may be caused by our approach of tracing electrons at the center energy of the E0 channel. Differences between the two sets of electromagnetic fields cause subtle discrepancies in the PADs near C/A, including a broader dropout at large pitch angles when using the fields from Fatemi et al. (2016) and a narrower range of electron fluxes near perpendicular pitch angles that only extends $\pm 20°$ beyond $\alpha = 90°$ when using the fields from Stahl et al. (2023b). However, the robustness of these results from both models presents strong support that such a pancake distribution is a key feature of Ganymede's energetic electron environment.

Besides capturing the pancake electron distribution near closest approach, both sets of fields also reproduce the dropout of electrons with $0° \leq \alpha \leq 20°$ outbound of 10:15 UTC that was observed by Galileo. These PADs indicate that EPD was on a field line with one end connected to Ganymede and the other open to Jupiter's magnetosphere. In addition, the models show a depletion of electrons with $\alpha \approx 90°$ from ∼9:45 UTC up until Galileo crossed through the mini-magnetosphere nearly 20 minutes later. This feature is not caused by gyrating electrons that impact Ganymede, since the gyroradius of an $E = 21$ keV electron in the ambient Jovian magnetospheric field is only on the order of 5 km, and the Galileo spacecraft was at least $1.5R_G$ away from the moon. Instead, both sets of models suggest a magnetic field magnitude that is slightly reduced in this region (i.e., before ∼10:05 UTC; see Fatemi et al., 2016; Stahl et al., 2023b), which,

due to conservation of the first adiabatic invariant, causes the electrons' velocities to become more field-aligned. Interestingly, these modeled signatures occur in the same region as the scattered beams that were measured by EPD, characterized by reduced flux across a broad range of pitch angles from $30° \lesssim \alpha \lesssim 150°$ (see Figure 1d). Although the morphology of the observed and modeled PADs is similar, the mechanisms generating these features may be different, especially if the beams originate from Jupiter's magnetosphere (Mauk & Saur, 2007). Regardless, our results provide evidence that Ganymede alters the energetic electron environment even at these distances.

To better understand the dynamics of electrons at Ganymede, and to identify whether the pancake distributions observed during G28 were associated with a trapped electron population, Figure 2 shows, in forward-time, the trajectory of one electron from a vantage point located in Ganymede's upstream, anti-Jovian hemisphere, as it travels through the electromagnetic fields from Fatemi et al. (2016). Figure 2a illustrates that this electron was traveling northward through Jupiter's magnetosphere with an energy of $E \approx$ 15 keV before it encountered Ganymede's interaction region. After initially entering the mini-magnetosphere along an open field line downstream of the moon (e.g., along recently reconnected magnetotail field lines), the electron crossed into the closed field line region and began drifting in a counterclockwise direction (when viewed from above), during which the particle mirrored multiple times near Ganymede's open/closed field line boundary. Figure 2 shows that this electron completed four full orbits of the moon in $\sim$ 13 minutes before escaping the mini-magnetosphere (see panel 2d). Throughout its orbit, the electron's energy periodically fluctuated depending on its position in the mini-magnetosphere, reaching an energy as large as 35 keV in the sub-Jovian hemisphere and as low as $\sim$ 10 keV in the anti-Jovian hemisphere. After the electron exited the mini-magnetosphere, its energy was a factor of $\sim$ 1.6 larger compared to when it entered.

To investigate the processes driving the dynamics of this electron, Figures 2e–j display various quantities along its orbit, for times when the particle's pitch angle was $\alpha =$ 90°. For the first $\sim$ 10 minutes of the particle's orbit, Figure 2 shows a correlation between $|\mathbf{B}|$ and the electron's energy. During this time the (relativistic) first adiabatic invariant μ remained nearly conserved, where $\mu = \gamma m |\mathbf{v}_\perp|^2/(2|\mathbf{B}|)$. Since Figure 2e–j displays only times when the electron's pitch angle was $\alpha = 90°$, the particle's perpendicular velocity $|\mathbf{v}_\perp|$ is equal to its total velocity $|\mathbf{v}|$, and hence, panel 2g displays its total (relativistic) kinetic energy. As such, for regions where μ was conserved and the elec-

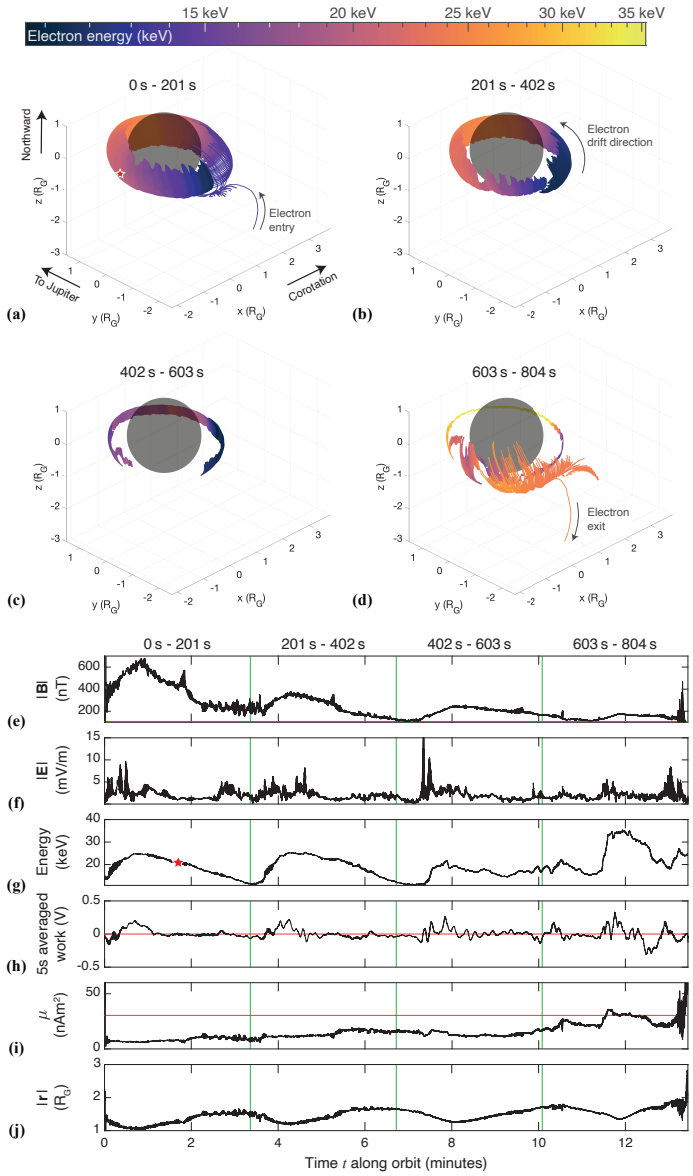

Figure 2. Trajectory of a trapped electron orbiting Ganymede. Panels (a–d) each display 201 s in real time (i.e., one-quarter of the complete displayed trajectory), colored corresponding to the electron's energy. Panels (e–j) display the local (e) magnetic and (f) electric field magnitudes, (g) electron's energy, (h) a five-second running average of the work ($-\mathbf{E} \cdot \mathbf{v}dt$) done on the electron, (i) first adiabatic invariant, μ, and (j) radial distance $|\mathbf{r}|$ at its mirror points when the electron's pitch angle is $\alpha = 90°$. The red stars in panels (a) and (g) show where the electron crossed Galileo's trajectory at 10:13 UTC with an energy of $E = 21$ keV and pitch angle of $\alpha = 120°$. Red horizontal lines denote the value of the respective quantity in the ambient Jovian magnetospheric plasma, while the green vertical lines split panels (e–j) into 201 s segments corresponding to panels (a–d).

tron traveled closer to Ganymede, its energy increased. There are additional regions during this initial ten-minute interval where μ was not conserved and the electron underwent a rapid energization, for example, approximately 7.5 minutes into its orbit. Here, $|\mathbf{E}|$ displayed a strong enhancement coinciding with an increase in the work done on the electron. These smaller energization events are associated with regions where the local electric field direction was aligned with the electron's motion, accelerating the particle through the fields (see panel 2h).

After this initial interval characterized by periodic acceleration and subsequent deceleration, an increase in the work done on the electron occurred nearly 11 minutes into its orbit. At this time, although any increase in $|\mathbf{E}|$ remained small, the electric field component parallel to the electron's velocity was enhanced (see Figure 2h) resulting in an increase in the work done on the electron and its rapid acceleration up to energies of $E \approx$ 35 keV. Near 12 minutes along its orbit, the particle's velocity vector became anti-aligned with the local electric field direction, the factor of two enhancement in energy that was gained from an electric field parallel to the electron's motion was lost, and the value of μ stabilized. However, one minute later (i.e., $\sim$ 13 minutes after becoming trapped in Ganymede's magnetic field), the electron experienced a strong enhancement in $|\mathbf{E}|$, conservation of the first adiabatic invariant broke down as μ became highly dynamic, and the particle was accelerated to an energy of $E \approx 25$ keV, after which the electron exited Ganymede's magnetosphere and traveled southward away from the moon in the Jovian magnetospheric field. The net energy gained by this electron therefore stemmed from work driven by an electric field parallel to the electron's velocity.

Such an energization mechanism for particles that may populate Ganymede's electron radiation belt supports the findings of Kollmann et al. (2022), who show that the electron PSD observed by EPD during G28 near closest approach was enhanced compared to just before and after C/A. If the PSD was associated with a stably trapped electron radiation belt, then it can not be explained through conservation of the first adiabatic invariant (i.e., not by the inward adiabatic transport of these electrons; see Kollmann et al., 2022). Instead, a local acceleration source is required (e.g., an electric field aligned with the electrons' velocities), which is consistent with the dynamics of the electron displayed in Figure 2. However, if the observation was driven by a more transient population, Kollmann et al. (2022) explain that the PSD observed during G28 may in-

stead be driven by impulsive electron transport through the local fields (as discussed for ions trapped in Jupiter's fields; see Kollmann et al., 2021).

Hence, to understand the significance of this single trapped electron's behavior in a statistical sense, we investigated the full trajectories of 1,728 electrons that were traced with GENTOo through the two sets of electromagnetic fields. These electrons represent a subset of those from the PADs in Figures 1e–f, but we focus only on three times when Galileo was within the closed field line region (at 10:06, 10:08, and 10:10 UTC), and subsample to a lower resolution of 15° in pitch angle and gyrophase. At these times, only electrons with initially near-perpendicular pitch angles had allowed trajectories (see Figures 1e–1f). Of the 864 back-traced electrons that we investigated from each set of fields at these three points, 7% had allowed trajectories when using the fields from Fatemi et al. (2016), while 28% were allowed when applying the fields from Stahl et al. (2023b). These percentages are comparable to the decrease in the electron differential energy flux observed by Galileo within the closed field line region (see Figure 1c). To determine the behavior of these electrons after encountering the G28 trajectory, we then traced these electrons beyond their "launch point" in *forward* time (i.e., $\mathrm{d}t > 0$). The back- and forward-traced segments were then combined to obtain the allowed electrons' complete trajectories near Ganymede.

Figure 3 shows the resulting electrons' lifetimes τ after entering within $r \leq 4R_G$ of Ganymede separated by their outcomes, either (blue) impacting Ganymede or (green) escaping the near-moon environment. Panel 3a displays the two outcomes for all electrons combined, while panel 3b separates them based on which set of electromagnetic fields were used. All of the electrons completed at least half of an orbit around Ganymede, with most entering the closed field line region from downstream of the moon. Moreover, 25% of these electrons (63 in the fields from Fatemi et al. (2016), including the electron in Figure 2, and another 13 in the fields from Stahl et al. (2023b)) completed *at least* one full orbit of the moon, with some encircling the moon multiple times. Half of these electrons that completed at least one orbit experienced a net acceleration by the time they impacted the surface or escaped Ganymede's local environment, compared to when they entered. Regardless of the electromagnetic field model used, Figure 3b indicates that the lifetimes for approximately 70% of electrons remain below $\tau \leq 3$ minutes (with medians of $1.0 \leq \tau \leq 1.7$ minutes). For the remaining 30%, the electrons traced through the fields from Fatemi et al. (2016) display longer lifetimes, with a maximum of $\tau \approx 30$

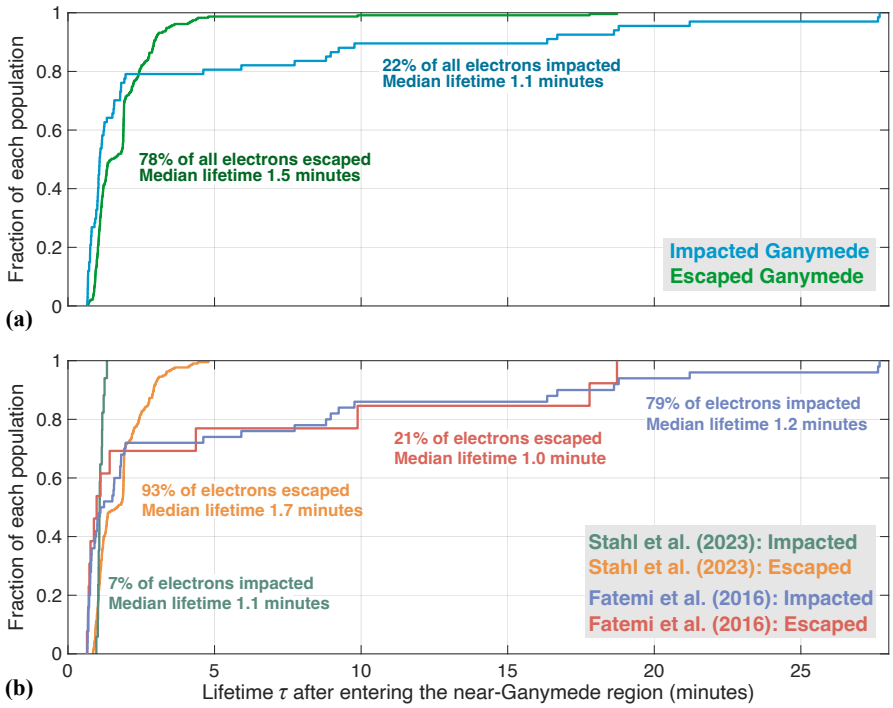

Figure 3. Lifetime τ of electrons as they pass by Ganymede. Fractions denote sub-populations corresponding to electrons that either impacted the surface or escaped the near-Ganymede environment. Panel (a) combines the outcome for all electrons traced, whereas panel (b) separates them based on the electromagnetic fields used for their tracing.

minutes, compared to those traced through the fields from Stahl et al. (2023b), with a maximum of $\tau \approx 5$ minutes.

4 Discussion and Conclusions

During the G28 Galileo flyby of Ganymede, EPD observed pancake distributions with for energetic electrons with enhanced fluxes near $\alpha \approx 90°$ compared to other pitch angles within the moon's closed field line region. Our results provide strong evidence that these electron PADs were associated with stably trapped electrons at the moon during this encounter. We have shown that they complete at least one half-orbit around Ganymede before impacting the surface or being lost to Jupiter's magnetosphere, with 25% of these electrons orbiting the moon at least once. We have identified similar behaviors for these particles when using two separate sets of electromagnetic fields to represent the perturbed plasma environment, providing confidence in the robustness of our results. Ganymede

can therefore efficiently trap electrons, sustain radiation belts for extended periods of time, and act as an acceleration mechanism for some electrons before they impact the surface or re-enter the Jovian magnetosphere. The differential azimuthal motion of this trapped electron population compared to energetic ions (which, unlike electrons, likely do not complete full orbits of the moon; see Poppe et al., 2018; Williams, 2001) may drive a partial ring current around Ganymede (see also Fatemi et al., 2022).

Using our approach, it is not feasible to further constrain the timescales over which trapped electrons are sustained to form radiation belts at the moon. The electron in Figure 2 orbited Ganymede for ~ 13 minutes, but our modeling indicates particles trapped for anywhere from 1 minute up to 30 minutes before they impact the surface or are lost to Jupiter's magnetosphere (see Figure 3). Ganymede's local environment is highly dynamic on these timescales and our present approach for modeling energetic electrons did not include various time-dependent processes (see also Collinson et al., 2018; Kaweeyanun et al., 2021; Kollmann et al., 2022; Mauk et al., 1997, 1999; Shprits et al., 2018). While these dynamics may represent a loss process for stable electron radiation belts, it is likely that they also act as a source for electrons to the mini-magnetosphere (e.g., via reconnection down-tail; see Eviatar et al., 2000). Future observations from the Particle Environment Package onboard JUICE (Galli et al., 2022) may encounter fluxes associated with this trapped population and should provide a unique opportunity to further characterize dynamics and lifetimes of these electrons.

Open Research

Galileo EPD data are available in Kollmann (2022), and the electromagnetic field outputs from the hybrid models used to trace electron dynamics are available in Liuzzo (2020) and Stahl et al. (2023a). Data from the GENTOo runs are available in Liuzzo (2024).

Acknowledgments

The authors are supported by NASA Solar System Workings grant 80NSSC21K0823 and L.L., A.R.P., and Q.N. acknowledge support from the France Berkeley Fund (fbf.berkeley.edu) grant number 15_2023. S.F. acknowledges support from the Swedish Research Council (VR) Grant 201803454. Computational resources were provided by the NASA High-End Computing Program through the NASA Advanced Supercomputing Division at Ames

Research Center. The authors thank two anonymous reviewers for comments which improved the manuscript.

References

Allioux, R., Louarn, P., & André, N. (2013, 4). Model of energetic populations at Ganymede, implications for an orbiter. *Advances in Space Research*, *51*(7), 1204–1212. doi: 10.1016/j.asr.2012.10.033

Collinson, G., Paterson, W. R., Bard, C., Dorelli, J., Glocer, A., Sarantos, M., & Wilson, R. (2018). New Results From Galileo's First Flyby of Ganymede: Reconnection-Driven Flows at the Low-Latitude Magnetopause Boundary, Crossing the Cusp, and Icy Ionospheric Escape. *Geophysical Research Letters*, *45*(8), 3382–3392. doi: 10.1002/2017GL075487

Cooper, J. F., Johnson, R. E., Mauk, B. H., Garrett, H. B., & Gehrels, N. (2001, 1). Energetic Ion and Electron Irradiation of the Icy Galilean Satellites. *Icarus*, *149*(1), 133–159. doi: 10.1006/icar.2000.6498

Eviatar, A., Williams, D. J., Paranicas, C., McEntire, R. W., Mauk, B. H., & Kivelson, M. G. (2000). Trapped Energetic Electrons in the Magnetosphere of Ganymede. *Journal of Geophysical Research: Space Physics*, *105*(A3), 5547–5553. doi: 10.1029/1999ja900450

Fatemi, S., Poppe, A. R., Khurana, K. K., Holmström, M., & Delory, G. T. (2016). On the formation of Ganymede's surface brightness asymmetries: Kinetic simulations of Ganymede's magnetosphere. *Geophysical Research Letters*, *43*(10), 4745–4754. doi: 10.1002/2016GL068363

Fatemi, S., Poppe, A. R., Vorburger, A., Lindkvist, J., & Hamrin, M. (2022). Ion Dynamics at the Magnetopause of Ganymede. *Journal of Geophysical Research: Space Physics*, *127*(1), 1–22. doi: 10.1029/2021JA029863

Galli, A., Vorburger, A., Carberry Mogan, S. R., Roussos, E., Stenberg Wieser, G., Wurz, P., ... Liuzzo, L. (2022). Callisto's Atmosphere and Its Space Environment: Prospects for the Particle Environment Package on Board JUICE. *Earth and Space Science*, *9*(5). doi: 10.1029/2021EA002172

Jia, X., & Kivelson, M. G. (2021, 4). The Magnetosphere of Ganymede. In *Magnetospheres in the solar system* (Vol. 2, pp. 557–573). doi: 10.1002/9781119815624.ch35

Kaweeyanun, N., Masters, A., & Jia, X. (2021). Analytical Assessment of Kelvin-Helmholtz Instability Growth at Ganymede's Upstream Magnetopause. *Journal of Geophysical Research: Space Physics*, *126*(8), 1–14. doi: 10.1029/2021JA029338

Kivelson, M., Khurana, K., & Volwerk, M. (2002, 6). The permanent and inductive magnetic moments of Ganymede. *Icarus*, *157*(2), 507–522. doi: 10.1006/icar.2002.6834

Kollmann, P. (2022). *Galileo EPD Calibrated Corrected Data Bundle.* [Dataset]. Planetary Data System. doi: 10.17189/n0dm-0014

Kollmann, P., Clark, G., Paranicas, C., Mauk, B., Haggerty, D., Rymer, A., & Allegrini, F. (2022). Ganymede's Radiation Cavity and Radiation Belts. *Geophysical Research Letters*, *49*(23), 1–10. doi: 10.1029/2022GL098474

Kollmann, P., Clark, G., Paranicas, C., Mauk, B., Roussos, E., Nénon, Q., ... Rymer, A. (2021). Jupiter's Ion Radiation Belts Inward of Europa's Orbit. *Journal of Geophysical Research: Space Physics*, *126*(4), 1–22. doi: 10.1029/2020JA028925

Liuzzo, L. (2020). *Data for "Energetic electron bombardment of Ganymede's surface" by Liuzzo et al., 2020.* [Dataset]. Zenodo. doi: 10.5281/zenodo.3754987

Liuzzo, L. (2024). *Data for "On the Formation of Trapped Electron Radiation Belts at Ganymede" by Liuzzo et al.* doi: 10.5281/zenodo.10780381

Liuzzo, L., Poppe, A. R., Addison, P., Simon, S., Nénon, Q., & Paranicas, C. (2022, 11). Energetic Magnetospheric Particle Fluxes Onto Callisto's Atmosphere. *Journal of Geophysical Research: Space Physics*, *127*(11), 1–30. doi: 10.1029/2022JA030915

Liuzzo, L., Poppe, A. R., Nénon, Q., Simon, S., & Addison, P. (2024). Constraining the Influence of Callisto's Perturbed Electromagnetic Environment on Energetic Particle Observations. *Journal of Geophysical Research: Space Physics*. doi: 10.1029/2023JA032189

Liuzzo, L., Poppe, A. R., Paranicas, C., Nénon, Q., Fatemi, S., & Simon, S. (2020, 9). Variability in the energetic electron bombardment of Ganymede. *Journal of Geophysical Research: Space Physics*, 1–35. doi: 10.1029/2020JA028347

Liuzzo, L., Simon, S., & Regoli, L. (2019a, 12). Energetic electron dynamics near Callisto. *Planetary and Space Science*, *179*(August), 104726. doi: 10.1016/j.pss

.2019.104726

Liuzzo, L., Simon, S., & Regoli, L. (2019b, 2). Energetic ion dynamics near Callisto. *Planetary and Space Science*, *166*, 23–53. doi: 10.1016/j.pss.2018.07.014

Mauk, B. H., & Fox, N. J. (2010, 12). Electron radiation belts of the solar system. *Journal of Geophysical Research: Space Physics*, *115*(A12), 1–19. doi: 10.1029/2010JA015660

Mauk, B. H., & Saur, J. (2007, 10). Equatorial electron beams and auroral structuring at Jupiter. *Journal of Geophysical Research: Space Physics*, *112*(A10). doi: 10.1029/2007JA012370

Mauk, B. H., Williams, D. J., & McEntire, R. W. (1997, 12). Energy-time dispersed charged particle signatures of dynamic injections in Jupiter's inner magnetosphere. *Geophysical Research Letters*, *24*(23), 2949–2952. doi: 10.1029/97GL03026

Mauk, B. H., Williams, D. J., McEntire, R. W., Khurana, K. K., & Roederer, J. G. (1999). Storm-like dynamics of Jupiter's inner and middle magnetosphere. *Journal of Geophysical Research: Space Physics*, *104*(A10), 22759–22778. doi: 10.1029/1999ja900097

Nénon, Q. (2022). *Galileo-EPD electron PADs.* [Dataset]. Figshare. doi: 10.6084/m9.figshare.20180222.v1

Nénon, Q., Miller, L. P., Kollmann, P., Liuzzo, L., Pinto, M., & Witasse, O. (2022, 8). Pitch Angle Distribution of MeV Electrons in the Magnetosphere of Jupiter. *Journal of Geophysical Research: Space Physics*, *127*(8), 1–21. doi: 10.1029/2022JA030627

Oran, R., Weiss, B. P., De Soria Santacruz-Pich, M., Jun, I., Lawrence, D. J., Polanskey, C. A., ... Elkins-Tanton, L. T. (2022). Maximum Energies of Trapped Particles Around Magnetized Planets and Small Bodies. *Geophysical Research Letters*, *49*(13), 1–11. doi: 10.1029/2021GL097014

Paranicas, C., Mauk, B. H., Kollmann, P., Clark, G., Haggerty, D. K., Westlake, J., ... Bolton, S. (2022, 5). Energetic charged particle fluxes relevant to Ganymede's polar region. *Geophysical Research Letters*. doi: 10.1029/2022GL098077

Plainaki, C., Massetti, S., Jia, X., Mura, A., Milillo, A., Grassi, D., ... Filacchione, G. (2020, 9). Kinetic Simulations of the Jovian Energetic Ion Cir-

culation around Ganymede. *The Astrophysical Journal*, *900*(1), 74. doi: 10.3847/1538-4357/aba94c

Plainaki, C., Massetti, S., Jia, X., Mura, A., Roussos, E., Milillo, A., & Grassi, D. (2022). The Jovian Energetic Ion Environment of Ganymede: Planetary Space Weather Considerations in View of the JUICE Mission. *The Astrophysical Journal*, *940*(2), 186. doi: 10.3847/1538-4357/ac9c54

Poppe, A. R., Fatemi, S., & Khurana, K. K. (2018, 6). Thermal and energetic ion dynamics in Ganymede's magnetosphere. *Journal of Geophysical Research: Space Physics*, *123*(6), 4614–4637. doi: 10.1029/2018JA025312

Roederer, J. G. (1967, 2). On the adiabatic motion of energetic particles in a model magnetosphere. *Journal of Geophysical Research*, *72*(3), 981–992. doi: 10.1029/jz072i003p00981

Schriver, D., Trávníček, P. M., Anderson, B. J., Ashour-Abdalla, M., Baker, D. N., Benna, M., ... Zurbuchen, T. H. (2011, 12). Quasi-trapped ion and electron populations at Mercury. *Geophysical Research Letters*, *38*(23), n/a-n/a. doi: 10.1029/2011GL049629

Shprits, Y. Y., Menietti, J. D., Drozdov, A. Y., Horne, R. B., Woodfield, E. E., Groene, J. B., ... Gurnett, D. A. (2018). Strong whistler mode waves observed in the vicinity of Jupiter's moons. *Nature Communications*, *9*(1), 7–12. doi: 10.1038/s41467-018-05431-x

Smith, B. A., Soderblom, L. A., Johnson, T. V., Ingersoll, A. P., Collins, S. A., Shoemaker, E. M., ... others (1979). The Jupiter system through the eyes of Voyager 1. *Science*, *204*(4396), 951–972. doi: 10.1126/science.204.4396.951

Stahl, A., Addison, P., Simon, S., & Liuzzo, L. (2023a). *Data for "Modeling of Ganymede's Magnetic and Plasma Environment During the Juno PJ34 Flyby" by Stahl et al. (2023).* [Dataset]. Zenodo. doi: 10.5281/zenodo.8370898

Stahl, A., Addison, P., Simon, S., & Liuzzo, L. (2023b, 12). A Model of Ganymede's Magnetic and Plasma Environment During the Juno PJ34 Flyby. *Journal of Geophysical Research: Space Physics*, *128*(12). doi: 10.1029/2023JA032113

Vorburger, A., Fatemi, S., Galli, A., Liuzzo, L., Poppe, A. R., & Wurz, P. (2022, 3). 3D Monte-Carlo simulation of Ganymede's water exosphere. *Icarus*, *375*(December 2021), 114810. doi: 10.1016/j.icarus.2021.114810

Williams, D. J. (2001). Ganymede's ionic radiation belts. *Geophysical Research Let-*

ters, *28*(19), 3793–3796. doi: 10.1029/2001GL013353

Williams, D. J. (2004). Energetic electron beams in Ganymede's magnetosphere. *Journal of Geophysical Research: Space Physics*, *109*(A9), 1–6. doi: 10.1029/2004JA010521

Williams, D. J., Mauk, B., & McEntire, R. W. (1997). Trapped electrons in Ganymede's magnetic field. *Geophysical Research Letters*, *24*(23), 2953–2956. doi: 10.1029/97GL03003